

1
2 **Systematic numerical investigation of the role of hierarchy in heterogeneous bio-**
3
4 **inspired materials**
5
6
7

8
9
10 Federico Bosia¹, Federico Della Croce² and Nicola M. Pugno^{3,4,5*}
11
12

13
14
15 ¹*Department of Physics and “Nanostructured Interfaces and Surfaces” Centre of Excellence,*
16
17
18 *University of Torino, 10125, Torino, Italy.*
19
20

21 ²*Department of Control and Computer Engineering, Politecnico di Torino, 10129, Torino, Italy.*
22
23

24 ³*Laboratory of Bio-Inspired Nanomechanics “Giuseppe Maria Pugno”, Department of Structural,*
25
26
27 *Geotechnical and Building Engineering, Politecnico di Torino, 10129, Torino, Italy.*
28

29 ⁴*National Institute of Nuclear Physics, National Laboratories of Frascati, Via E. Fermi 40, 00044,*
30
31
32 *Frascati, Italy.*
33
34

35 ⁵*National Institute of Metrological Research, Strada delle Cacce 91, I-10135, Torino, Italy.*
36
37
38

39
40
41 **Corresponding author: nicola.pugno@polito.it*
42
43
44
45
46
47

48
49 **Paper submitted to Special Issue of JMBBM**
50

51 **“Science and engineering of natural materials: Merging structure and material”**
52
53
54
55
56
57
58
59
60
61
62
63
64
65

Abstract:

1
2 It is well known that hierarchical structure is an important feature in biological materials to
3
4 optimize various properties, including mechanical ones. It is however still unclear how these
5
6 hierarchical architectures can improve material characteristics, for example strength. Also, the
7
8 transposition of these structures from natural to artificial bioinspired materials remains to be
9
10 perfected. In this paper, we introduce a numerical method to evaluate the strength of fibre-based
11
12 heterogeneous biological materials and systematically investigate the role of hierarchy. Results
13
14 show that hierarchy indeed plays an important role and that it is possible to “tune” the strength of
15
16 bio-inspired materials in a wide range of values, in some cases improving the strength of non
17
18 hierarchical structures considerably.
19
20
21
22
23
24
25
26
27
28
29
30
31
32
33
34
35
36
37
38
39
40
41
42
43
44
45
46
47
48
49
50
51
52
53
54
55
56
57
58
59
60
61
62
63
64
65

1. Introduction

1
2
3 It is known that many biological materials and organisms display fascinating physical and
4
5 mechanical properties, which have up to now been hard to replicate in artificial materials and
6
7 systems. One of these is the ability to combine exceptional strength and toughness, which occurs for
8
9 example in nacre, bone and dentine (Espinosa et al., 2011; Pugno, 2006; Wegst and Ashby, 2004),
10
11 or the smart adhesion which is found in spiders and geckos (Autumn et al., 2000; Autumn and
12
13 Peattie, 2002; Foelix, 1996; Tian et al., 2006). An important feature underlying these properties is
14
15 thought to be material structure and hierarchy (Fratzl and Weinkamer, 2007; Lakes, 1993). A prime
16
17 example of this is spider silk, whose hierarchical structure ranges from nanostructure to
18
19 macrostructure and consists of an amorphous network of chains and β -sheet crystals constituted by
20
21 poly-(Gly-Ala) and poly-Ala domains (Ackbarow et al., 2007; Keten et al., 2010). Molecular
22
23 dynamics and atomistic simulations have shown how the specific structure and bonding at
24
25 molecular level affects macroscopic properties like strength and toughness (Bratzel and Buehler,
26
27 2012; Keten et al., 2010; Nova et al., 2010).
28
29
30
31
32
33
34
35
36
37

38
39 Aside from spider silk, a great number of biological materials are inherently structurally
40
41 hierarchical. The hierarchical structure of tendon, taken from (Riley, 2005) is shown in Fig1a.
42
43 Another example is the case of bone, where variability at the nanometer level lies in the shape and
44
45 size of mineral particles, at the micron level in the arrangement of mineralized collagen fibers into
46
47 lamellar structures, and beyond in the inner architecture, the porosity and the shape of the bone.
48
49 Various studies show the dependence of the mechanical properties of bone on all these parameters
50
51 (Currey, 2002; Gibson et al., 1995; Launey et al., 2010; Rho et al., 1998; Weiner and Wagner,
52
53 1998). Other biological systems that have been studied to assess the role of hierarchy are tendons
54
55 (Puxkandl et al., 2002), protein materials (Gao, 2006), Gecko adhesion (Yao and Gao, 2006), tissue
56
57
58
59
60
61
62
63
64
65

growth (Cranford and Buehler, 2011).

1
2 Given a hierarchical organization, various designs are possible, by altering the type and
3
4 arrangement of the components at different levels. Hierarchy and functional grading frequently lead
5
6 to variable mechanical properties at different length scales, i.e. overall mechanical properties are
7
8 often quite different from those of constituents (Lakes, 1993; Pugno, 2006), and many natural
9
10 materials can be considered an equivalent of artificial composite materials. For example, stiff
11
12 biological materials are often composites with the smallest components mostly in the nanometer
13
14 range (Gao and Ji, 2004). In the case of plants or insect cuticles, a polymeric matrix is reinforced by
15
16 stiff polymer fibers, such as cellulose or keratin (Vincent, 1999), and in the case of bone or dentin
17
18 even stiffer structures are obtained using a fibrous polymeric matrix reinforced by hard carbonated
19
20 hydroxylapatite particles (Currey, 1999).
21
22
23
24
25
26
27
28

29 One possible hypothesis is therefore that the exceptional mechanical behavior of biological
30
31 materials is due to two essential elements: hierarchy and material heterogeneity. To verify this
32
33 conjecture, a number of theoretical models which include both these elements have been
34
35 formulated, including molecular dynamics or atomistic simulations (Buehler et al., 2009; Currey,
36
37 1999, 2003; Gao and Ji, 2004; Pugno, 2006). A simplified numerical approach is the fiber bundle
38
39 model (FBM) which has been extensively studied during the past years (Pradhan et al., 2010). This
40
41 model consists of a set of parallel fibers having statistically distributed strengths. The sample is
42
43 loaded parallel to the fiber direction, and the fibers fail if the load exceeds their threshold value,
44
45 with the load carried by the broken fiber being redistributed among the intact ones. The Equal Load
46
47 Sharing (ELS) formulation is most often adopted, whereby after each fiber break the stress is
48
49 equally distributed on the intact fibers, neglecting stress concentrations in the vicinity of failed
50
51 regions. Based on this model, we developed a hierarchical formulation of the FBM (“HFBM”) and
52
53
54
55
56
57
58
59
60
61
62
63
64
65

1 used it to calculate the space elevator cable strength including the role of defects (Pugno et al.,
2 2008). With this model we also studied the strength and toughness of nanotube-based composites,
3
4 starting from the properties and volume fractions of the fragile and ductile constituents (Bosia et al.,
5 2010). In recent work, we addressed the issue of the synergy between hierarchy and material mixing
6
7 to enhance the mechanical performance of composites, finding evidence that some hierarchical
8
9 configurations lead to an improvement with respect to the non hierarchical case (Bosia et al., 2012)
10
11 An important numerical study of damage evolution in hierarchical FBMs was also recently carried
12
13 out by Mishnaevsky (Mishnaevsky, 2011).
14
15
16
17
18
19
20

21 However, despite the recent advances in this field, a systematic study addressing the role of
22
23 *pure* hierarchy (independently of the specific material system it refers to), its interaction with
24
25 material heterogeneity, and their effect on macroscopic mechanical properties is still missing. In this
26
27 paper, we therefore wish to begin such a systematic study, and investigate the possibility of tuning
28
29 and optimizing the strength of hierarchical fibre bundles composed of different fibre types as a
30
31 function of hierarchy and distribution of different fibre types.
32
33
34
35
36
37

38 The paper is structured as follows: in Section 2, we introduce the numerical model used to
39
40 calculate the strength of hierarchical fiber bundle architectures in composite materials and the
41
42 evaluation procedure; in Section 3, we present results of calculations and their discussion; finally,
43
44 conclusions and outlook are given.
45
46
47
48

49 **2. Hierarchical Fibre Bundle Model**

50 *2.1 Model implementation*

51
52
53 As mentioned above, a Hierarchical Fibre Bundle Model (HFBM) was adopted for simulations. The
54
55 model used here is related to that proposed by Bosia *et al.* (Bosia et al., 2008) and Pugno *et al.*
56
57 (Pugno et al., 2008). As with all FBMs, the individual fibres have randomly-assigned statistically-
58
59
60
61
62
63
64
65

distributed strengths, in our case according to the 2 parameter Weibull distribution (see Fig.2),
which is described by the following equation (Weibull, 1939, 1951):

$$P(\sigma) = 1 - e^{-\left(\frac{\sigma}{\sigma_0}\right)^m} \quad (1)$$

The model is based on an Equal-Load-Sharing (ELS) FBM approach, replicated in a hierarchical scheme at various length scales (“levels”) to predict from statistical considerations the mechanical behaviour of different hierarchical architectures. Also, in order to model heterogeneous fibrous media, the fibres of each bundle can assume different mechanical properties. The k -th fibre type is characterized by a Young’s modulus E_k , length l_k , cross-sectional area A_k , and Weibull-distributed fracture strengths, the latter characterized by a scale parameter σ_{0k} and shape parameter m_k . The various types of fibres combine in forming bundles, with complex mechanical behaviour emerging from the mechanical properties and arrangement of the constituent fibres. The specimen’s stress-strain behaviour is determined by imposing an increasing displacement and “rupturing” individual fibres in the bundle (i.e. setting their stiffness to zero) when their statistically assigned strength is exceeded. After each fracture event, the load is redistributed uniformly among the fibres in the same bundle as the fractured one (ELS). The bundle strength is obtained as the maximum stress value reached in the simulation before failure, i.e. when all parallel fibres of the bundle have failed. Since the fibre strengths are assigned randomly according to the Weibull distribution, results differ for each simulation, and average trends can be derived from repeated simulations.

Hierarchy is implemented as described by Pugno et al. (Pugno et al., 2008) and Bosia et al. (Bosia et al., 2008), schematically illustrated in Fig.3, i.e. the input mechanical behaviour of a level $i=h-1$ “fibre” or subvolume is statistically inferred from the output deriving from hundreds of level

1
2
3
4
5
6
7
8
9
10
11
12
13
14
15
16
17
18
19
20
21
22
23
24
25
26
27
28
29
30
31
32
33
34
35
36
37
38
39
40
41
42
43
44
45
46
47
48
49
50
51
52
53
54
55
56
57
58
59
60
61
62
63
64
65

h simulations, that of a level $i=h-2$ subvolume from level $i=h-1$ simulations, and so on, down to the lowest hierarchical level $i=1$. Overall, the specimen is modelled as an ensemble of N_1 subvolumes arranged in a bundle. Each of these subvolumes is in turn constituted by N_2 subvolumes, arranged in a bundle as before. This scheme is applied for h “generations”, up to a level h subvolume, which is constituted N_a type “ a ” fibres, N_b type “ b ” fibres, and so on.

Since at every single fibre failure the load is only redistributed among parallel fibres in the “local” bundle, fibre failures in different bundles “interact” only at the next hierarchical level. Thus, comparing hierarchical bundles with the same overall number of fibres and fibre-type percentages, but different hierarchical architectures, amounts to considering different stress redistribution schemes in the material. To simplify the problem, we initially consider only 2 fibre types (a and b , basically a “matrix” and a “reinforcement” as in composites) and symmetrical structures (each bundle is split into identical bundles at each hierarchical level). Thus, to define the overall bundle, we require the following parameters:

i. Fixed parameters:

N (integer): total number of fibres

E_a and E_b (real number): stiffnesses for fibres a and b

σ_a and σ_b (real number): Weibull scale parameters for fibres a and b

m_a and m_b (real number): Weibull shape parameters for fibres a and b

α (real number): Fraction of type a fibres, so that $(1-\alpha)$ is the fraction of type b fibres. $0 < \alpha < 1$

ii. Variable parameters:

h (integer): number of hierarchical levels

n_1, n_2, \dots, n_{h-1} (integers): number of parallel bundles at hierarchical levels $i=1, 2, \dots, (h-1)$

n_a (integer): number of parallel bundles of type a fibres at the last hierarchical level $i=h$

n_b (integer): number of parallel bundles of type b fibres at the last hierarchical level $i=h$

Clearly, for $h>1$, any configuration with $n_i=1$ corresponds to a $(h-1)$ architecture, e.g. a $h=3$ configuration with $n_1=1, n_2=2, n_a=5, n_b=10$ is identical to $h=2, n_1=2, n_a=5, n_b=10$. Therefore, for $h>1$, only configurations with $n_i>1$ are considered.

The number of free parameters depends on the number of hierarchical levels of the considered structures. Two equivalent parameters are the number of type a and b fibres, respectively, in each bundle at level h , i.e. $N_a = \frac{\alpha N}{n_1 n_2 \dots n_{i-1} n_a}$ and $N_b = \frac{(1-\alpha)N}{n_1 n_2 \dots n_{i-1} n_b}$. The only constraints on the variable parameters are thus that N_a and N_b must be integers. To be able to satisfy this constraint, N needs to be sufficiently large, however this increases computational time, so a compromise is required (typically $N=10^2 \div 10^4$). To avoid excessively time-consuming problems, we can consider initially $h<4$. Each simulation is repeated typically 10^2 times to obtain a mean strength for the considered structure.

To illustrate the procedure, let us consider an example of a 3-level hierarchical structure ($h=3$) with $N=3600$ and $\alpha=0.2$. The chosen mechanical parameters are $E_a=1000$ GPa and $E_b=10$ GPa for the Young's moduli, and $\sigma_a=100$ GPa $\sigma_b=1$ GPa, $m_a=2, m_b=3$ for the Weibull scale and shape parameters, respectively. One possible structure with these parameters is shown in Fig.3a. Each "box" in the figure represents a fibre bundle. N_i indicates the number of fibres in each bundle at hierarchical level i . A fibre bundle at hierarchical level i is equivalent to a single fibre at hierarchical level $i-1$. The distinction between fibres a and b occurs only at the highest hierarchical level $i=h$. We observe here that a rule of mixtures (Gibson, 2007) for this non-hierarchical configuration yields a strength value of 18.44 GPa. This is because the rule of mixtures is strictly valid only in the case of simultaneous failure of all fibres in the bundle, which does not occur because of the statistical distribution of the fibre strengths. Typically, in this study the non-hierarchical bundle reaches its

1
2 maximum stress (i.e. strength value) when about 50% of its constituent fibres (both a and b) have
3 failed, leading to the cited strength value of about 9.1 GPa. Consequently, the rule of mixtures is
4 only an upper bound for the mean strength, and does not provide a reliable estimation method in
5 this case.
6
7
8
9

10 The strength of hierarchical structures with the same fixed parameters (specified above) is thus
11 compared to the non-hierarchical ($h=0$) fibre bundle (Fig.3b), the “default configuration”, where all
12 fibres are in parallel ($N=3600$, $N_a=720$, $N_b=2880$). The latter configuration has a mean strength of
13 9.1 GPa. In order to evaluate the variation of bundle strength with hierarchy level and type, all
14 possible configurations are systematically considered for $h=1, 2$ and 3 . The number of possible
15 configurations for the given parameters are 1260 for $h=1$, 4690 for $h=2$, and 8641 for $h=3$,
16 respectively. These numbers are calculated numerically for by determining all n_1 (and n_2 if $h=3$), n_a
17 and n_b values that give rise to integer values for N_a and N_b . Since single-fibre strengths are
18 randomly assigned based on a Weibull distribution, there is some variability in results for each
19 given configuration. Thus, simulations are repeated 10^2 times for each configuration and a mean
20 value and standard deviation are calculated.
21
22
23
24
25
26
27
28
29
30
31
32
33
34
35
36
37
38
39
40
41
42

43 *2.2 Hierarchical configuration analysis*

44
45 Regarding the number of possible configurations for given N and α parameters, some general
46 considerations can be made. Given an even number N of springs, if we denote by \hat{h} the maximum
47 number of levels allowed for N , this number is at most the total number of prime factors (distinct or
48 not) of N . On the other hand, the total number $T(N)$ of different configurations must take into
49 account the number of levels $l=2\dots\hat{h}$ and for each level l all related configurations. As explained
50 above, at least two fibres must be present in each bundle at every level, or else the configuration
51
52
53
54
55
56
57
58
59
60
61
62
63
64
65

must be considered as belonging to the lower hierarchical level. $T(N)$ is significantly larger than N already for a limited value of \hat{h} . Indeed, if we consider the case where N is a power of 2 (namely $N=2^{\hat{h}}$) and $\alpha=0.5$, then we have \hat{h} prime factors all equal to 2 and $\alpha N = (1-\alpha)N = 2^{\hat{h}-1}$. Hence, as N_a and N_b must be integers, we have a feasible configuration if the product $n_1 \cdot n_2 \cdot \dots \cdot (n_l - 1) = 2^j$ for any integer $j = 1, \dots, \hat{h} - 1$, where $l = 1, \dots, j$ denotes the number of levels of this configuration. Notice that, as $n_1 \cdot n_2 \cdot \dots \cdot (n_l - 1)$ are all integers, they are also a power of 2. Correspondingly, the total number of different combinations such that $n_1 \cdot n_2 \cdot \dots \cdot (n_l - 1) = 2^j$ summed on all values of $l = 1, \dots, j$ is exactly 2^j . On the other hand, given j , $N_a = \frac{2^{\hat{h}-j-1}}{n_a}$ and $N_b = \frac{2^{\hat{h}-j-1}}{n_b}$. Hence n_a and n_b can each have any value 2^x with $x = 0, 1, \dots, \hat{h} - j - 1$. That is, for any given j the number of different combinations of n_a and n_b is given by $(\hat{h} - j)^2$. Overall, by summing upon all $j = 1, \dots, \hat{h} - 1$, we have that, for $N = 2^{\hat{h}}$, $T(N) = \sum_{j=1}^{\hat{h}-1} 2^j (\hat{h} - j)^2$. For instance, for $N = 4096 = 2^{13}$, we have $T(N) = \sum_{j=1}^{12} 2^j (13 - j)^2 = 48756$. When N is not a power of 2, the analysis becomes more tedious while the combinatorial explosion is even larger. Just to give a rough idea on the matter, if we suppose one wants to compute the number of different configurations with $\alpha=0.5$, $n_a = n_b = 1$ and number of levels $t = \hat{h}$: then, when the prime factors of N are all identical (as for $N=2^{\hat{h}}$), there is just one configuration. On the other hand, when the prime factors of N are all distinct, for any t -uple of these different factors assigned to t different levels, there are $t!$ different assignments of such factors to the levels (namely all possible permutations of a string with length t) correspondingly inducing $t!$ different combinations.

Based on these observations, for the chosen value of N , the required calculation time for $h \geq 4$ becomes unacceptable, so that in further studies global optimization techniques have to be implemented to maximize strength or other required properties.

3. Results

3.1 Influence of hierarchy

First, we consider the case where only one type of fibre is present, i.e. $\alpha = 1$, to evaluate the influence of hierarchy only. The mean strength in the non hierarchical case here is 43.1 GPa). The allowable configurations are evaluated numerically for the chosen N and h parameters by determining all n_l and n_a values that give rise to integer values for N_a . The numbering of the configurations is chosen so as to have increasing n_l values as first criterion, and increasing n_a values as second. Figure 4 illustrates the calculations for the mean strength of the various hierarchical configurations for $h=2$. A quasi-periodic behaviour is found, related to the n_l value (as highlighted in Fig.4b). Maximum strength is obtained when maximizing n_a values, for given n_l values, and the overall maximum strength value is obtained when maximizing both n_l and n_a (49.7 GPa). This corresponds to hierarchical architectures where bundles constituted of a minimal number of fibres are present, i.e. where minimum stress redistribution occurs in the material in the fracture process. In 9 cases the non-hierarchical mean strength is exceeded, although values are affected by some fluctuations, due to the statistical nature of the simulations.

3.2 Influence of hierarchy and fibre mixing

Next, to additionally evaluate the influence of material heterogeneity together with hierarchy, let us consider a “mixed” bundle with $N=3600$ and $\alpha = 0.2$. As explained above, the strength of various different hierarchical structures is evaluated for $h=1, 2, 3$. It is important to remember that some statistical variability remains in these data, as simulations are based on randomly assigned single-fibre strengths for fibre types a and b . Thus, while calculation results do not provide an absolute comparison between different configurations, results are strongly indicative of the relative strength

1
2
3
4
5
6
7
8
9
10
11
12
13
14
15
16
17
18
19
20
21
22
23
24
25
26
27
28
29
30
31
32
33
34
35
classification. Mean strength results for $h=1$ structures are shown in Fig.5. The x -axis represents the considered configurations (again ordered according to increasing n_a), whilst the corresponding strength is plotted on the y -axis in log scale. In this case, the parameters n_a and n_b are sufficient to define the structure, i.e. the different configurations are obtained by simply changing the number of bundles of fibres of type a and b , since only a single level of hierarchy is present. It is found that in this case hierarchy does not favour maximal strength, because the maximum value (8.71 GPa) is obtained for $[n_a=1, n_b=1]$ (configuration number 1260 in Fig.5), which corresponds to the non-hierarchical case. However, many other “hierarchical” configurations generate similar strength values, and appear as local maxima in the plot in Fig.5. These favourable configurations are those where the number of parallel fibres is maximized, both for type a and type b fibres, i.e. when n_a and n_b are small and/or not too dissimilar in value. Conversely, the minima appear for large values of n_a or n_b , especially if one of the two exceeds a limiting value (e.g. n_a or $n_b > 720$). This is highlighted more clearly in Fig.6, where strength values are plotted vs. n_a and n_b in a 3-D plot.

36
37
38
39
40
41
42
43
44
45
46
47
48
49
50
51
52
From Figs. 5 and 6 it is apparent that the choice of hierarchical arrangement can lead to a variation in strength of more than an order of magnitude. These observations lead to the consideration that appropriate choice of fibre arrangements can provide the means to obtain tailor-made strength properties, starting from the same constituents. No strength improvement is obtained with respect to the non-hierarchical arrangement, proving that higher-level hierarchy is a key factor in this respect.

53
54
55
56
57
58
59
60
61
62
63
64
65
Results for $h=2$ are shown in Fig.7. Here, the number of available configurations is greater (a total of 4690), as a function of the additional parameter n_l . For each given n_l value, the same quasi-periodic behaviour as in Figs. 4 and 5 is observed as a function of n_l , with maximum strength values obtained for simultaneous large values of n_a and n_b and a similar excursion between maxima

1 and minima. Thus, these results are consistent with those for $\alpha=1$ (single fibre type) and $h=2$, and
2 are in contrast with those for $\alpha=0.2$ and $h=1$. This once again proves the importance of hierarchy in
3 determining a qualitatively different behaviour. Here, for increasing n_I values, the number of
4 available (n_a, n_b) pairs decreases, so that the number of evaluated configurations also decreases and
5 with it the “period” of the oscillations. The number of configurations with a mean strength greater
6 than the non-hierarchical case is 28, with a maximum value of 10.1 GPa, so the introduction of fibre
7 mixing improves the situation with respect to the single-fibre case.
8
9

10 The results obtained with the chosen fibre fraction $\alpha=0.2$ are qualitatively confirmed for
11 different α values. For example, the case $\alpha=0.5$ is considered (Fig.8). Clearly, for this α value, the
12 overall mean strength increases because of the larger fraction of “strong” fibres (type a), and the
13 mean strength in the non-hierarchical case is 21.8 GPa. Again, a quasi-periodic behaviour is
14 obtained in the configuration space, with the best configurations occurring for various n_I values
15 when maximizing n_a and n_b values, which corresponds to the cases of greatest of "local" stress
16 redistributions. Some variability remains, due to the statistical nature of the simulations. A greater
17 number of configurations (66) provide an improvement with respect to the non-hierarchical case,
18 with a maximum mean strength value of 26.4 GPa (a 21% improvement). Results are compared in
19 Tables 1 and 2 for $h=2$ and $\alpha=0.2$ and $\alpha=0.5$, respectively.
20
21
22
23
24
25
26
27
28
29
30
31
32
33
34
35
36
37
38
39
40
41
42
43
44
45

46 As shown in Fig.9, results are more complicated for $h=3$. There remains an oscillating quasi-
47 periodic behaviour as a function of the hierarchical configuration, with local maxima and minima,
48 as a function of the n_I, n_2, n_a and n_b values. As seen in Table 3, where the 10 most favourable
49 configurations are reported, the maxima in mean strength can be found in configurations where at
50 least one of these numbers is maximized, in particular the n_a value, relative to the “strong” type a
51 fibres, so the analysis for $h=2$ is confirmed. Similar to lower-order hierarchies, maximal attained
52
53
54
55
56
57
58
59
60
61
62
63
64
65

1
2 strength values exceed the non hierarchical case (9.1 GPa) in 34 cases, i.e. a smaller number of
3 cases with respect to $h=2$ and $\alpha = 0.5$. This seems to indicate that hierarchical structure is all the
4 more effective for greater high-strength fibre content percentage.
5
6

7 To better analyze these qualitative indications, a systematic study for higher hierarchical levels
8 needs to be carried out. For $h>3$, it is not possible to analyze all configurations, due to
9 computational time, but preliminary data (not reported) shows that the overall tendency highlighted
10 at $h=1, 2, 3$ seems to continue, with a greater span between minimal and maximal strength values,
11 and the more favourable configurations being close to those where the number of parallel fibres at
12 level h is maximized.
13
14
15
16
17
18
19
20
21
22
23
24
25
26

27 **4. Conclusions**

28 We have presented a systematic procedure to evaluate the influence of heterogeneity and
29 hierarchy in fibre bundle architectures using a Hierarchical Fibre Bundle Model. The first three
30 hierarchical levels have been investigated and a considerable strength variability as a function of
31 hierarchical configuration has been highlighted, with a mean strength improvement of up to 21%
32 with respect to the non hierarchical case. The hierarchical configurations with better strength
33 characteristics are those favouring the more spatially confined stress redistributions during fracture.
34 The results in this paper are promising for the improvement of the performance of artificial bio-
35 inspired architectures and the design of materials with tailor made properties. To derive more
36 specific and quantitative conclusions, in future a wider investigation of the parameter space will be
37 carried out. A greater number of hierarchical levels will be assessed, using global optimization
38 techniques to avoid exceedingly cumbersome calculations and the emphasis will be particularly on
39 metaheuristics based on local improvement techniques (Gendreau and Potvin, 2010). Also, other
40
41
42
43
44
45
46
47
48
49
50
51
52
53
54
55
56
57
58
59
60
61
62
63
64
65

properties will be investigated, including stiffness and energy dissipation, in order to address the problem of the simultaneous optimization of different material properties (e.g. strength and toughness), which is a commonplace feature in nature but remains to be effectively achieved in artificial materials.

Acknowledgements

This work is supported by the ERC Ideas Starting grant n. 279985 “BIHSNAM, Bio-inspired Hierarchical Super Nanomaterials”, which is gratefully acknowledged.

References

- 1
2
3 Ackbarow, T., Chen, X., Keten, S., Buehler, M.J., 2007. Hierarchies, multiple energy barriers, and
4
5 robustness govern the fracture mechanics of alpha-helical and beta-sheet protein domains.
6
7
8 Proceedings of the National Academy of Sciences of the United States of America 104, 16410-
9
10 16415.
11
12
13 Autumn, K., Liang, Y.A., Hsieh, S.T., Zesch, W., Chan, W.P., Kenny, T.W., Fearing, R., Full, R.J.,
14
15 2000. Adhesive force of a single gecko foot-hair. Nature 405, 681-685.
16
17
18 Autumn, K., Peattie, A.M., 2002. Mechanisms of adhesion in geckos. Integrative and Comparative
19
20 Biology 42, 1081-1090.
21
22
23 Borgia, F., Abdalrahman, T., Pugno, N.M., 2012. Investigating the role of hierarchy on the strength
24
25 of composite materials: evidence of a crucial synergy between hierarchy and material mixing.
26
27
28 Nanoscale 4, 1200-1207.
29
30
31 Borgia, F., Buehler, M.J., Pugno, N.M., 2010. Hierarchical simulations for the design of supertough
32
33 nanofibers inspired by spider silk Physical Review E 82, 056103.
34
35
36 Borgia, F., Pugno, N., Lacidogna, G., Carpinteri, A., 2008. Mesoscopic modeling of Acoustic
37
38 Emission through an energetic approach. International Journal of Solids and Structures 45, 5856-
39
40 5866.
41
42
43 Bratzel, G., Buehler, M.J., 2012. Sequence-structure correlations in silk: Poly-Ala repeat of N.
44
45 clavipes MaSp1 is naturally optimized at a critical length scale. Journal of the Mechanical Behavior
46
47 of Biomedical Materials 7, 30-40.
48
49
50 Buehler, M.J., Qin, Z., Cranford, S., Ackbarow, T., 2009. Robustness-Strength Performance of
51
52 Hierarchical Alpha-Helical Protein Filaments. International Journal of Applied Mechanics 1, 85-
53
54 112.
55
56
57
58
59
60
61
62
63
64
65

1
2 Cranford, S.W., Buehler, M.J., 2011. Shaky foundations of hierarchical biological materials. *Nano*
3 *Today* 6, 332-338.
4
5 Currey, J.D., 1999. The design of mineralised hard tissues for their mechanical functions. *Journal of*
6 *Experimental Biology* 202, 3285-3294.
7
8 Currey, J.D., 2002. *Bones : structure and mechanics*. Princeton University Press, Princeton, NJ.
9
10 Currey, J.D., 2003. How well are bones designed to resist fracture? *Journal of Bone and Mineral*
11 *Research* 18, 591-598.
12
13 Espinosa, H.D., Juster, A.L., Latourte, F.J., Loh, O.Y., Gregoire, D., Zavattieri, P.D., 2011. Tablet-
14 level origin of toughening in abalone shells and translation to synthetic composite materials. *Nature*
15 *Communications* 2.
16
17 Foelix, R.F., 1996. *Biology of spiders*, 2nd ed. Oxford University Press ; Georg Thieme Verlag,
18 New York [Stuttgart].
19
20 Fratzl, P., Weinkamer, R., 2007. Nature's hierarchical materials. *Progress in Materials Science* 52,
21 1263-1334.
22
23 Gao, H.J., 2006. Application of fracture mechanics concepts to hierarchical biomechanics of bone
24 and bone-like materials. *International Journal of Fracture* 138, 101-137.
25
26 Gao, H.J., Ji, B.H., 2004. Mechanical properties of nanostructure of biological materials. *Journal of*
27 *the Mechanics and Physics of Solids* 52, 1963-1990.
28
29 Gendreau, M., Potvin, J.-Y., 2010. *Handbook of metaheuristics*, 2nd ed. Springer, New York.
30
31 Gibson, L.J., Ashby, M.F., Karam, G.N., Wegst, U., Shercliff, H.R., 1995. *The Mechanical-*
32 *Properties of Natural Materials* .2. Microstructures for Mechanical Efficiency. *Proceedings of the*
33 *Royal Society of London Series a-Mathematical and Physical Sciences* 450, 141-162.
34
35 Gibson, R.F., 2007. *Principles of composite material mechanics*, 2nd ed. CRC Press, Boca Raton.
36
37
38
39
40
41
42
43
44
45
46
47
48
49
50
51
52
53
54
55
56
57
58
59
60
61
62
63
64
65

1 Keten, S., Xu, Z.P., Ihle, B., Buehler, M.J., 2010. Nanoconfinement controls stiffness, strength and
2 mechanical toughness of beta-sheet crystals in silk. *Nature Materials* 9, 359-367.
3
4 Lakes, R., 1993. *Materials with Structural Hierarchy*. *Nature* 361, 511-515.
5
6
7 Launey, M.E., Buehler, M.J., Ritchie, R.O., 2010. On the Mechanistic Origins of Toughness in
8 Bone. *Annual Review of Materials Research*, Vol 40 40, 25-53.
9
10
11
12 Mishnaevsky, L., 2011. Hierarchical composites: Analysis of damage evolution based on fiber
13 bundle model. *Composites Science and Technology* 71, 450-460.
14
15
16
17
18 Nova, A., Keten, S., Pugno, N.M., Redaelli, A., Buehler, M.J., 2010. Molecular and Nanostructural
19 Mechanisms of Deformation, Strength and Toughness of Spider Silk Fibrils. *Nano Letters* 10, 2626-
20 2634.
21
22
23
24
25
26 Pradhan, S., Hansen, A., Chakrabarti, B.K., 2010. Failure processes in elastic fiber bundles.
27 *Reviews of Modern Physics* 82, 499-555.
28
29
30
31 Pugno, N.M., 2006. Mimicking nacre with super-nanotubes for producing optimized super-
32 composites. *Nanotechnology* 17, 5480-5484.
33
34
35
36
37 Pugno, N.M., Bosia, F., Carpinteri, A., 2008. Multiscale stochastic simulations for tensile testing of
38 nanotube-based macroscopic cables. *Small* 4, 1044-1052.
39
40
41
42
43 Puxkandl, R., Zizak, I., Paris, O., Keckes, J., Tesch, W., Bernstorff, S., Purslow, P., Fratzl, P., 2002.
44 Viscoelastic properties of collagen: synchrotron radiation investigations and structural model.
45 *Philosophical Transactions of the Royal Society of London Series B-Biological Sciences* 357, 191-
46 197.
47
48
49
50
51
52
53
54 Rho, J.Y., Kuhn-Spearing, L., Zioupos, P., 1998. Mechanical properties and the hierarchical
55 structure of bone. *Medical Engineering & Physics* 20, 92-102.
56
57
58
59
60 Riley, G., 2005 Chronic tendon pathology: molecular basis and therapeutic implications *Expert*
61
62
63
64
65

Reviews in Molecular Medicine 7, 1-25.

1
2 Tian, Y., Pesika, N., Zeng, H.B., Rosenberg, K., Zhao, B.X., McGuiggan, P., Autumn, K.,
3

4
5 Israelachvili, J., 2006. Adhesion and friction in gecko toe attachment and detachment. Proceedings
6
7 of the National Academy of Sciences of the United States of America 103, 19320-19325.
8
9

10 Vincent, J.F.V., 1999. From cellulose to cell. Journal of Experimental Biology 202, 3263-3268.
11

12
13 Wegst, U.G.K., Ashby, M.F., 2004. The mechanical efficiency of natural materials. Philosophical
14
15 Magazine 84, 2167-2181.
16
17

18 Weibull, W., 1939. A statistical theory of the strength of materials. Ingeniörsvetenskapsakademiens
19
20 Handlingar 151.
21
22

23
24 Weibull, W., 1951. A statistical distribution function of wide applicability. Journal of Applied
25
26 Mechanics -Transactions ASME 18, 293–297.
27
28

29
30 Weiner, S., Wagner, H.D., 1998. The material bone: Structure mechanical function relations. Annual
31
32 Review of Materials Science 28, 271-298.
33
34

35
36 Yao, H., Gao, H., 2006. Mechanics of robust and releasable adhesion in biology: Bottom-up
37
38 designed hierarchical structures of gecko. Journal of the Mechanics and Physics of Solids 54, 1120-
39
40 1146.
41
42
43
44
45
46
47
48
49
50
51
52
53
54
55
56
57
58
59
60
61
62
63
64
65

List of Figure Captions

1 Fig.1: a) Hierarchical structure of tendon (from (Riley, 2005)), b) Schematization of the
2
3 hierarchical procedure in multiscale simulations
4
5

6 Fig.2: Two-parameter Weibull distribution $p(\sigma)$ for the strength distribution of level-0 fibres in the
7
8 FBM: σ_0 is the scale parameter and m is the shape parameter (in this case $m=2$)
9
10

11 Fig.3: a) Schematization of an example of a 3-level hierarchical structure; b) Schematization of the
12
13 corresponding reference non-hierarchical structure.
14
15
16

17 Fig4.: a) Simulations results for the mean strength of different fibre arrangements for $h=2$ and $\alpha=1$;
18
19 b) close-up on the first 250 configurations, highlighting the quasi-periodic dependency on the n_1
20
21 index. The dotted line indicates the mean strength value for the non-hierarchical case.
22
23
24

25 Fig.5: Simulations results for the mean strength of different fibre arrangements for $h=1$ and $\alpha=0.2$.
26
27 The dotted line indicates the mean strength value for the non-hierarchical case.
28
29
30

31 Fig.6: 3-D plot of mean strength simulations results for $h=1$ and $\alpha=0.2$
32
33

34 Fig.7: Mean strength simulations results for $h=2$ and $\alpha=0.2$. The dotted line indicates the mean
35
36 strength value for the non-hierarchical case.
37
38

39 Fig.8: Mean strength simulations results for $h=2$ and $\alpha=0.5$.
40
41

42 Fig.9: Mean strength simulations results for $h=3$ and $\alpha=0.2$
43
44
45
46

List of Table captions

47
48
49 Table 1: Examples of configurations providing maxima in mean strength for $h=2$ simulations, with
50
51 $\alpha=0.2$.
52
53
54

55 Table 2: Examples of configurations providing local maxima in mean strength for $h=2$ simulations,
56
57 with $\alpha=0.5$
58
59
60

61 Table 3: Maxima in mean strength for $h=3$ simulations, with $\alpha=0.2$
62
63
64
65

Figure 1
[Click here to download high resolution image](#)

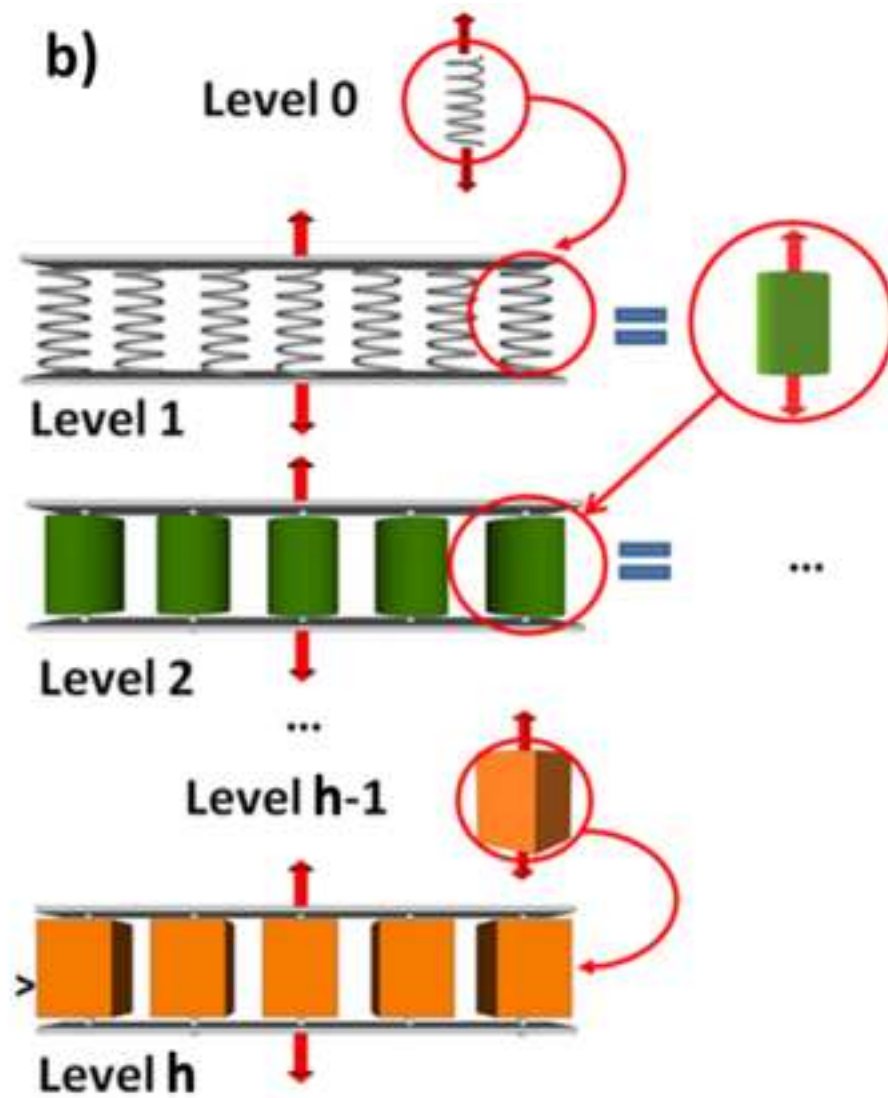
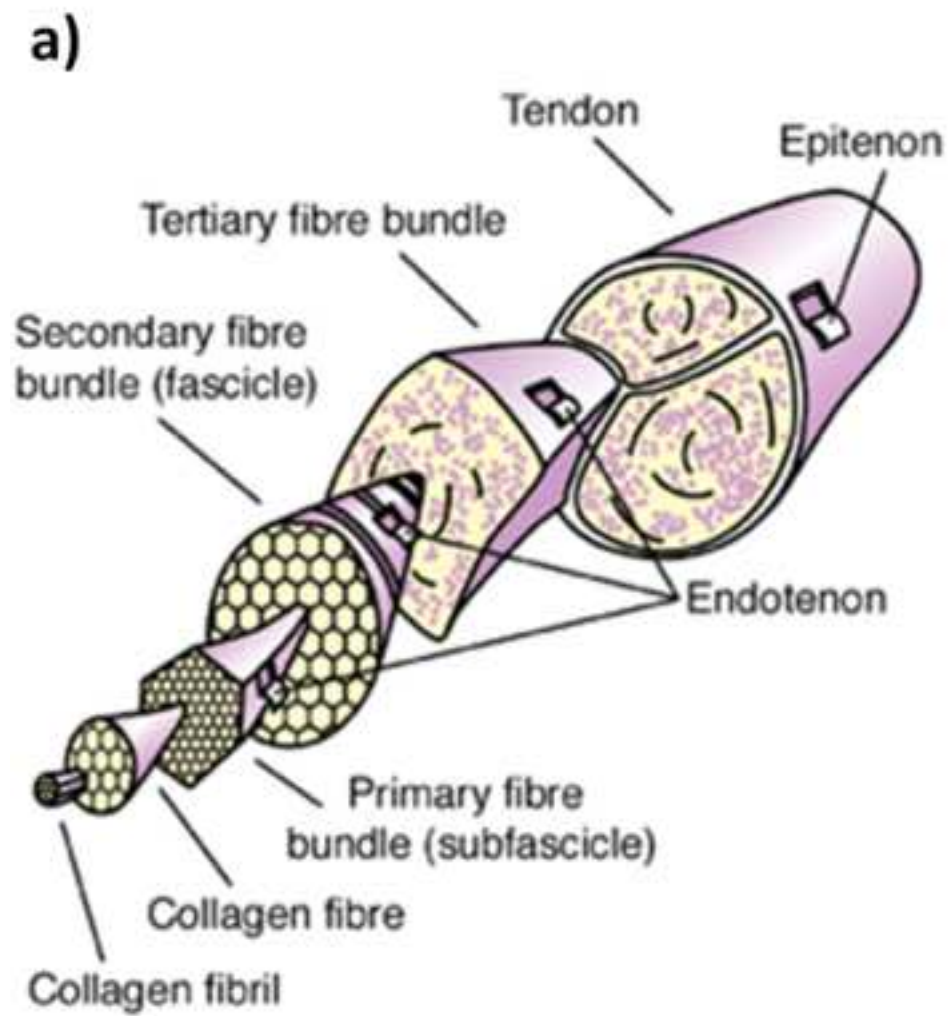


Figure 2
[Click here to download high resolution image](#)

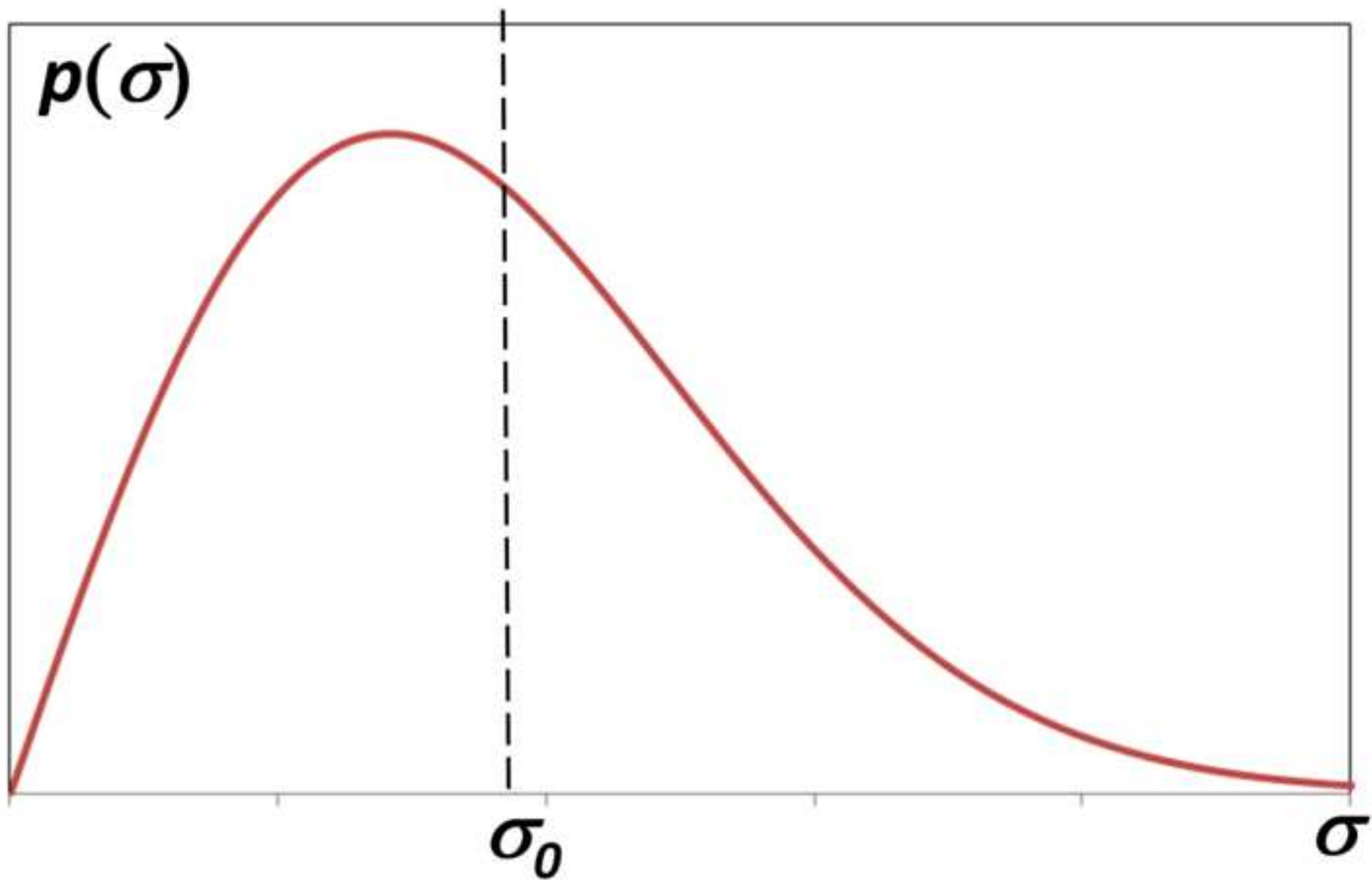


Figure 3
[Click here to download high resolution image](#)

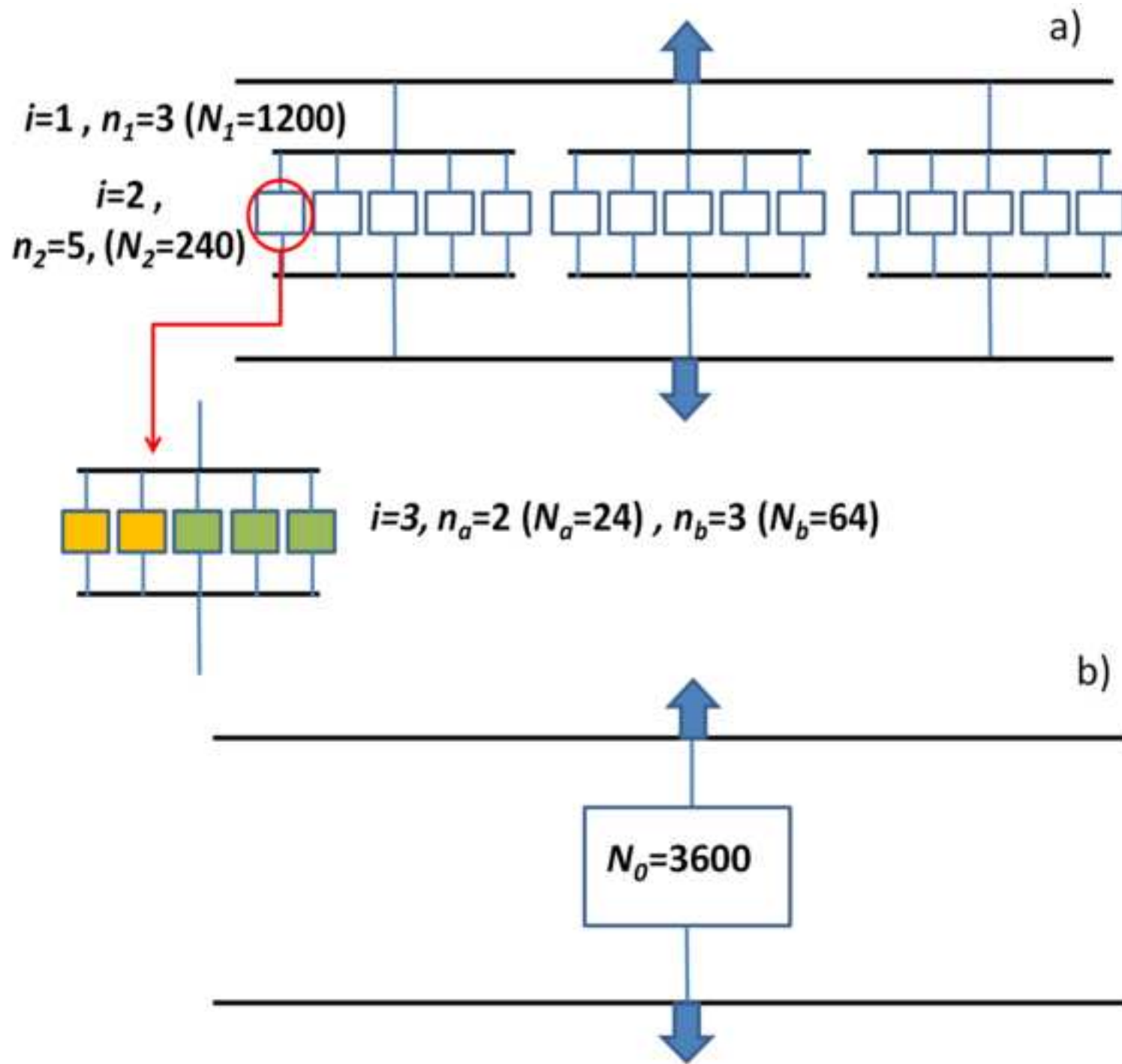


Figure 4
[Click here to download high resolution image](#)

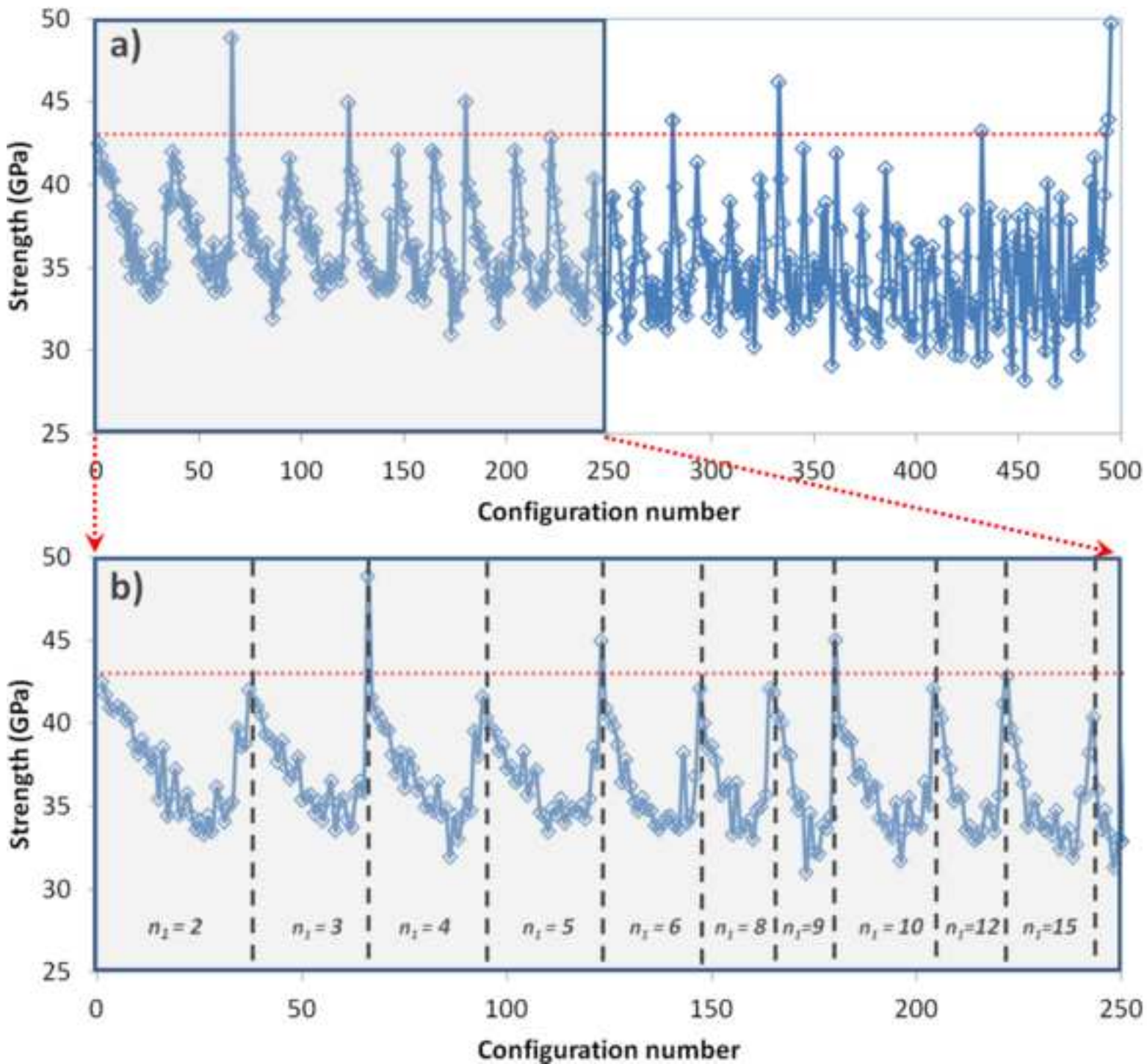


Figure 5
[Click here to download high resolution image](#)

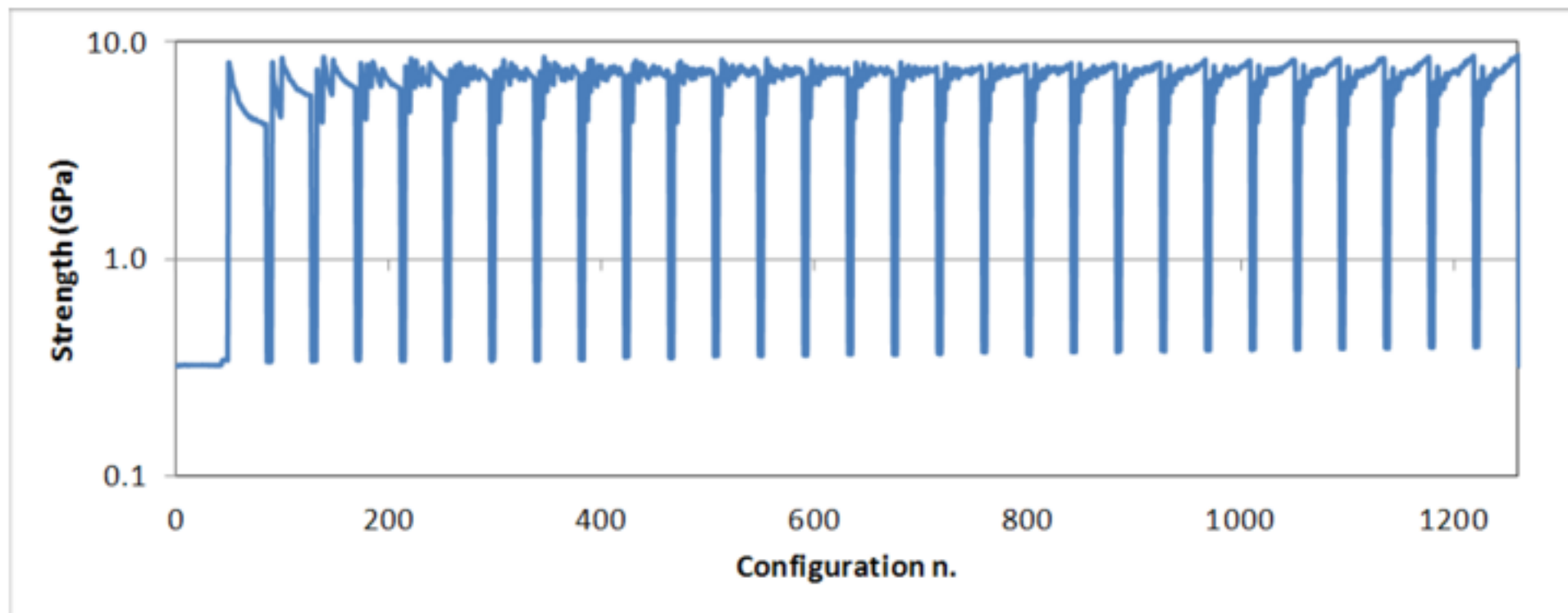


Figure 6
[Click here to download high resolution image](#)

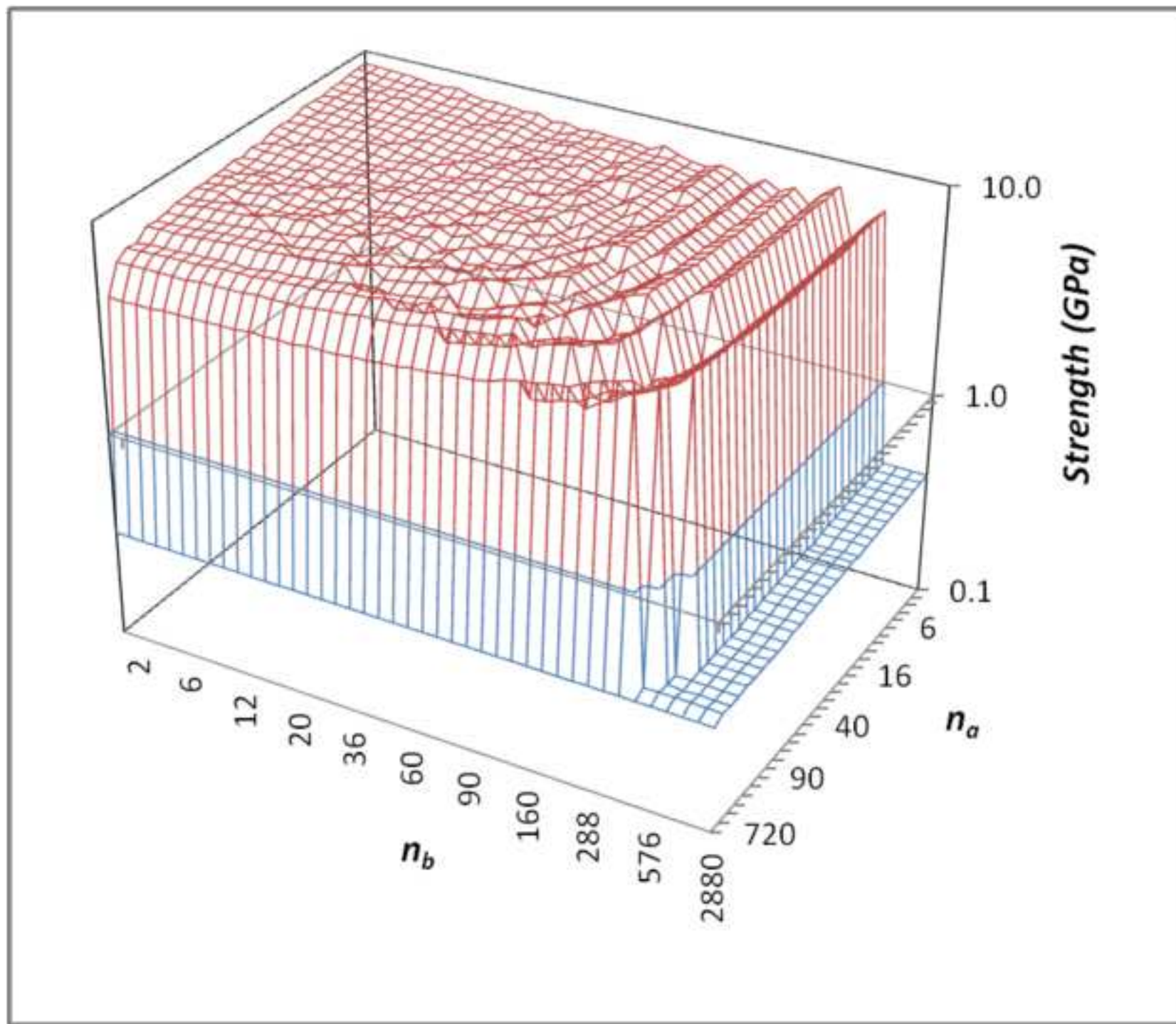


Figure 7
[Click here to download high resolution image](#)

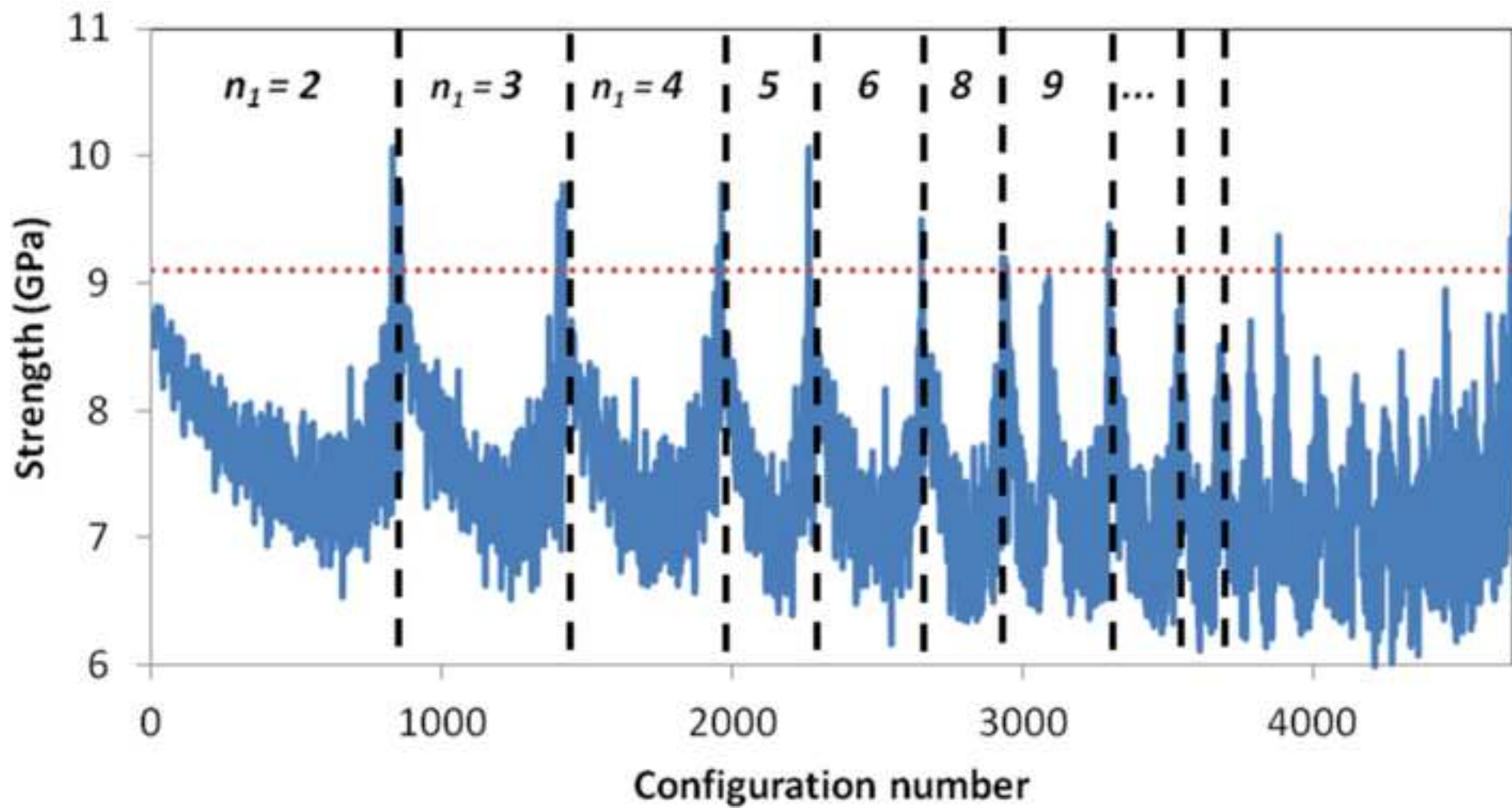


Figure 8
[Click here to download high resolution image](#)

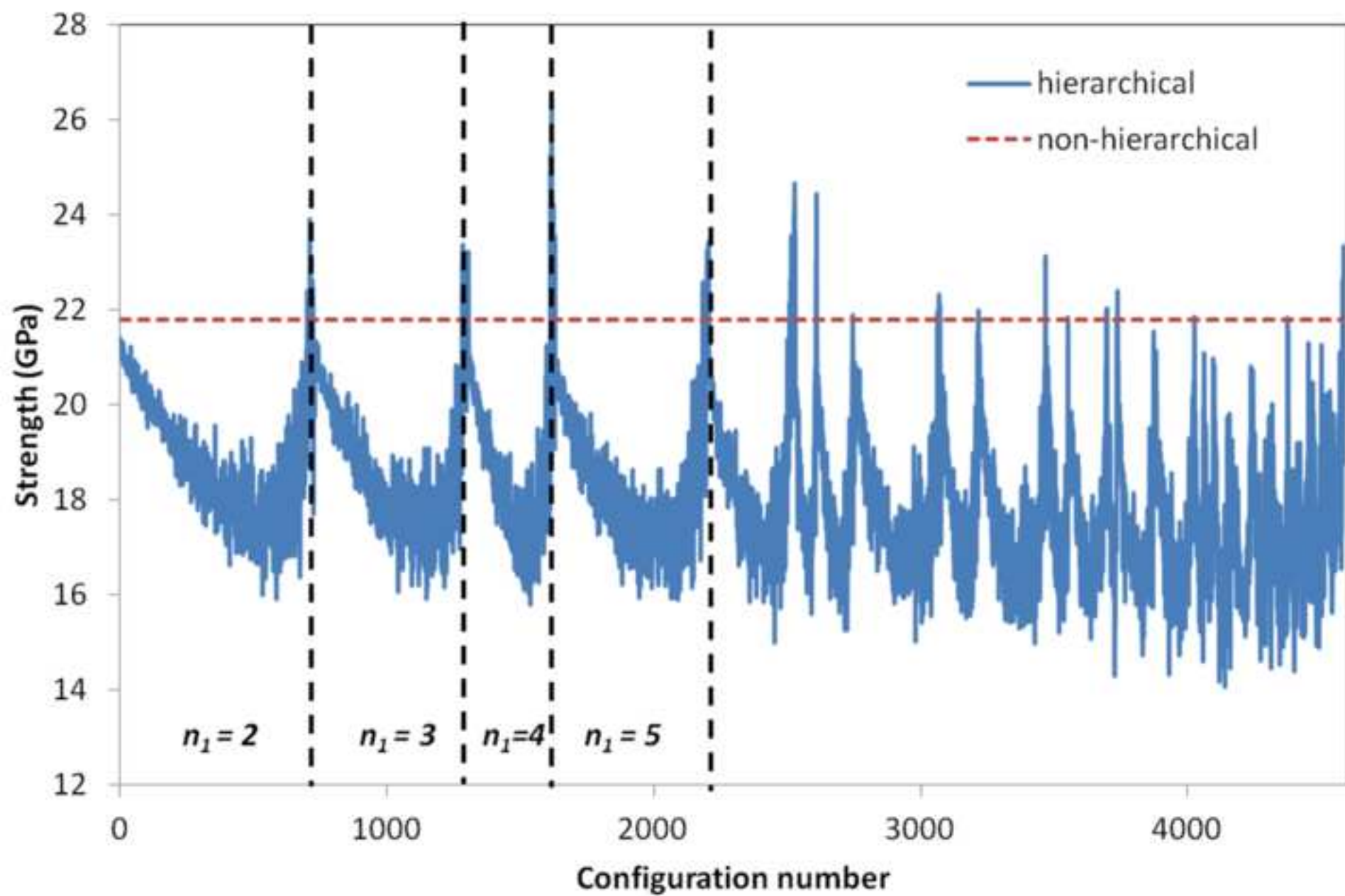
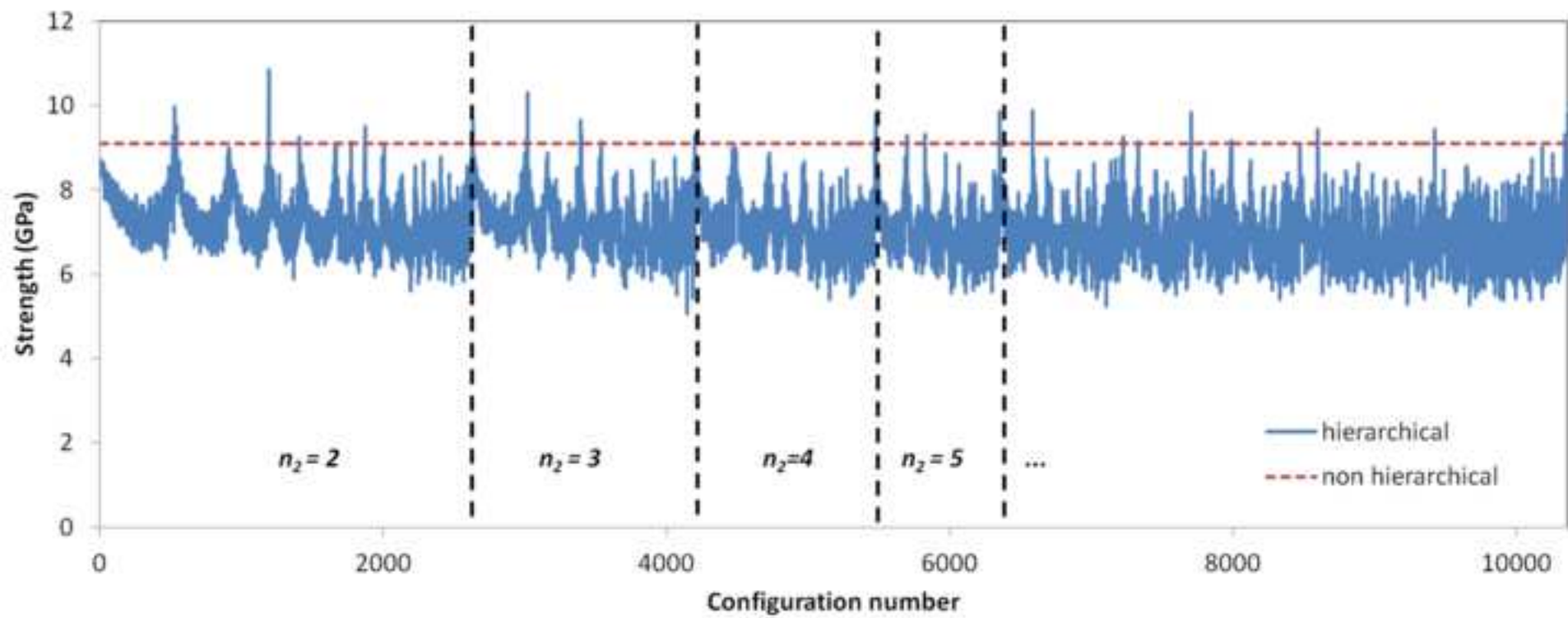


Figure 9
[Click here to download high resolution image](#)



Tables

Table 1

n_l	n_a	n_b	Strength (GPa)
5	144	144	10.07
2	360	720	10.07
2	360	20	9.81
3	240	12	9.78
2	360	10	9.76
4	180	2	9.75
3	240	192	9.64
3	240	6	9.63
3	240	64	9.57
720	1	1	9.57

Table 2

n_l	n_a	n_b	Mean Strength (GPa)
4	450	9	26.4
4	450	2	25.2
6	300	100	24.6
8	225	75	24.4
4	450	45	24.2
6	300	60	24.0
2	900	12	23.9
6	300	300	23.6
6	300	3	23.6
4	450	450	23.5

Table 3

Configuration n.	n_1	n_2	n_a	n_b	Mean Strength (GPa)
1192	2	4	90	4	10.8
3020	3	2	120	480	10.3
527	2	2	180	36	10.0
6582	6	2	60	6	9.9
6354	5	144	1	1	9.9
7704	8	90	1	4	9.8
5480	4	180	1	2	9.8
10359	360	2	1	2	9.8
3393	3	4	60	24	9.7
2634	2	360	1	1	9.6